Characterizing Non-linear Fatigue Crack Growth and Size Effect in Plain Concrete Beams with a Hybrid Effective Crack and Cohesive Zone Model

Nicholas Andres Brake and Karim Chatti

Abstract The mechanical response of concrete is largely influenced by the inter-locking coarse aggregate, which supplies the cement matrix with a resisting cohesive crack bridging force. Under low and high cycle fatigue loading, the cohesive stresses can influence the crack growth rate and the structural load capacity. A new method used to quantify the cyclic cohesive zone properties and effective crack resistance in three point bending single edge notch plain concrete specimens of different sizes under both low and high cycle fatigue loading is presented here. For validation, three point bend concrete specimens of two different sizes were tested under crack mouth opening displacement controlled low cycle quasi-static loading and force controlled high cycle fatigue using constant, variable, and random amplitude loading sequences. The results indicate that the cohesive stress-dependent cyclic crack resistance can be quantified and used to effectively characterize the high cycle fatigue non-linear crack growth and size effect.

Keywords Concrete fatigue · R-curve · Size effect · Random loading

1 Introduction

Concrete is a quasi-brittle material that exhibits 'small crack' behavior; the cohesive stresses acting along the concrete crack face strongly influence the fracture characteristics of the material, e.g., the fatigue crack propagation rate and fracture toughness. Plain concrete is made of relatively large aggregates which engender a

N.A. Brake
Department of Civil and Environmental Engineering, Lamar University,
Beaumont, USA
e-mail: nicholas.brake@lamar.edu

K. Chatti (✉)
Department of Civil and Environmental Engineering, Michigan State University,
East Lansing, USA
e-mail: chatti@egr.msu.edu

proportionally large cohesive stress zone near the crack tip (Cox and Marshall 1991) and is responsible, in large part, for the size effect and R-curve behavior (Fett et al. 2000), crack deceleration region in fatigue (Li and Matsumoto 1998) and influencing the endurance limit (Kruzic et al. 2005). Several researchers investigated the relationship between cohesive stresses and size effect (Bazant and Kazemi 1990; Morel 2007; Roesler et al. 2007), and its relationship to the R-curve (Foote et al. 1986; Mai 2002; Bazant and Cedolin 1984; Gallops et al. 2011). In fatigue loading concrete experiences non-linear crack growth, where it initially decelerates and gradually accelerates until failure (Brake and Chatti 2012; Subramaniam et al. 2000).

In pavement engineering, a new mechanistic empirical design protocol was recently launched to predict damage caused by millions of traffic and environmental loadings. The high cycle fatigue damage model is based on an empirical SN curve and a linear damage rule (Miner 1945). Fatigue SN models, although computationally efficient, are limited in that they cannot capture non-linear damage accumulation, size, and the R-ratio effect. A simple but yet powerful alternative approach could be to use a modified Paris law that can capture non-linear crack growth, load history, and size effects. Most importantly, the Paris law is still very computationally efficient in that the number of cycles to failure can be predicted by evaluating a simple integral (Bazant and Planas 1998). However, there is a need for a computationally efficient model that can predict plain concrete non-linear crack growth, size effect, and load capacity under various loading sequences. This paper presents such a model.

2 Model Framework

The model proposed in this paper uses an LEFM framework that considers constant and variable amplitude loading and non-linear crack growth. The model uses a modified Paris law that incorporates the use of a fatigue resistance curve to simulate the effects of cohesive stresses on crack growth. The inclusion of the cohesive stresses can significantly reduce the size dependency observed in Paris constant: C and n, in Portland cement concrete (PCC). The cohesive stresses are described with a fatigue R-curve for computational efficiency; the relationship between the cohesive stresses and fatigue R-curve are shown in Table 1 from Brake and Chatti (2013). Equation 1 shows the modified Paris equation. The variables a and

Table 1 Dimensionally consistent regression equations

$K_{Rc}^f = 0.228 K_{IC}^T + 0.1677, R^2 = 0.95$	$\Delta a_c = 6.377 \times 10^{-5} \left(\frac{w_c E}{K_{IC}^T}\right)^2 + 0.603, R^2 = 0.97$
$\frac{\lambda_1}{\sqrt{D}} = 3.074 \frac{f_t'}{D} + 0.025, R^2 = 0.89$	$\lambda_2 = -1.053 \frac{D}{l_{ch}} + 0.025, R^2 = 0.89$
$K_{IC}^T = \sqrt{G_F^T E}, G_F^T = \int_0^{w_c} \sigma_{coh}(\delta) d\delta$	$l_{ch} = \left(\frac{K_{IC}^T}{f_t'}\right)^2$

N represents the crack length and cycle number, respectively. The variable K_I is the mode-I stress intensity given in Eqs. 2 and 3, K_R^F is the fatigue crack resistance curve, σ_N is the nominal stress at mid-span, D is the beam depth, b is the beam width, $k(\alpha)$ is the stress intensity geometric correction factor given in Eq. 4, α is the non-dimensional crack length (a/D), P is the applied load at mid-span, and S is the beam span

$$\frac{da}{dN} = C\left(K_I - K_R^f\right)^n \tag{1}$$

$$K_I = \sigma_N \sqrt{D} k(\alpha) \tag{2}$$

$$\sigma_N = \frac{3PS}{2bD^2} \tag{3}$$

The stress intensity geometric correction factor for a three–point bending single end notch (TPBSEN) specimen with a span to depth ratio (S/D) of 4 is shown in Eq. 4.

$$k(\alpha) = \frac{\sqrt{\alpha}[1.99 - \alpha(1 - \alpha)(2.15 - 3.93\alpha + 2.7\alpha^2)]}{(1 + 2\alpha)(1 - \alpha)^{3/2}} \tag{4}$$

The resisting curve function is governed by five variables: K_{Rc}^f, Δa_c, m, λ_1, and λ_2 as shown in Eq. 5. The first three parameters govern the shape of the pre-peak region and the last two govern the post-peak slope. To maintain first order continuity, the functions must be connected at the equivalent crack length, which can be calculated with Eqs. 6 and 7.

$$K_R^f = \left\{ \begin{array}{ll} K_{RC}^f\left[1 - \left(1 - \frac{\Delta a}{\Delta a_c}\right)^m\right], & 0 \leq \Delta a < \Delta a_\beta \\ K_{\beta c}^f + \beta(\Delta a - \Delta a_\beta), & \Delta a \geq \Delta a_\beta \end{array} \right\} \tag{5}$$

where

$$\Delta a_\beta = \left(1 - \left(\frac{\beta \Delta a_c}{mK_{Rc}^f}\right)^{\frac{1}{m-1}}\right)\Delta a_c, m > 1, \frac{\beta \Delta a_c}{mK_{Rc}^f} < 1 \tag{6}$$

$$\beta = \lambda_1 \exp\left[\lambda_2 \frac{\Delta P}{P\max}\right] \tag{7}$$

These parameters are related to the cohesive stress function shown in Eq. 8 using the empirical regression equations shown in Table 1 from (Brake and Chatti 2013), where f'_t is the concrete tensile strength, w_c is the crack opening displacement at

zero stress, and c_1 and c_2 are shape parameters. K_{IC}^T is the total fracture toughness, G_F^T is the total fracture energy, and l_{ch}, is the characteristic length.

$$\sigma_{coh}(\delta(x)) = f_t' \left\{ \left[1 + \left(\frac{c_1 \delta(x)}{w_c} \right)^3 \right] \exp\left(-\frac{c_2 \delta(x)}{w_c} \right) - \left(\frac{\delta(x)}{w_c} \right) (1 + c_1^3) \exp(-c_2) \right\}$$

(8)

A series of fatigue experiments were conducted to determine the Paris constants from Eq. 1 and to determine their statistical significance with regards to specimen size and loading sequence.

3 Experimental Program

3.1 Materials

The concrete was made of ASTMC-150 Type I cement, natural sand, and a limestone coarse aggregate (nominal maximum size of 25 mm). The water to cement ratio was 0.45 and the air content was 6.5 %. The 28 day compressive strength was 25 MPa. The beam specimens were allowed to cure for one year inside of a humidity room, and were removed one month prior to testing. The average split tensile strength and compressive strength at the time of testing was 3.79 and 40.62 MPa, respectively.

3.2 Notched Three Point Bending Tests

The beams were subjected to (i) quasi-static loading, (ii) constant amplitude fatigue loading, (iii) variable amplitude fatigue loading, and (iv) random amplitude fatigue loading. The span to depth ratio was 4. Beams with two different depths were tested: 50 and 100 mm; where the width, b, was equal to the depth, d, in all the beams. The beams were tested under three different notch-depth ratios: 0.15, 0.33, and 0.5 (Fig. 1).

A total of 48 plain PCC three point bend specimens were tested; six were tested under low cycle quasi-static loading and 34 tested under high cycle fatigue loading. The specimens tested under quasi-static loading were loaded and un-loaded at a COD controlled rate of 0.0005 mm/s until ultimate failure. Under high cycle fatigue loading, the specimens were subjected to constant, variable, and random amplitude loading sequences. Each load was applied at a frequency of 2 Hz. For the constant amplitude tests, stress ratios (SR) between 0.95 and 0.8 and an R-ratio of 0.05 were applied. The compliance and equivalent crack was measured at each loading cycle
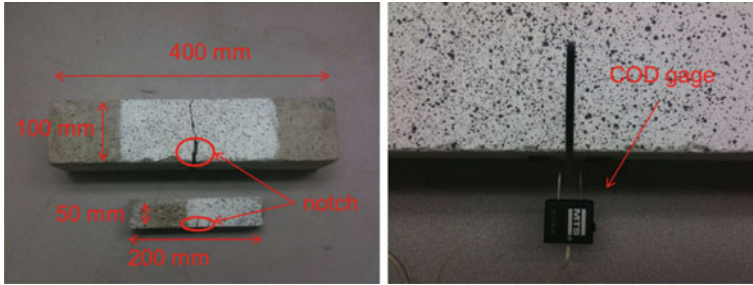
Fig. 1 Photograph of the two different beam sizes, notch, and COD gage

using peak-to-peak crack mouth opening displacement (CMOD) measurements (Jenq and Shah 1985). Equations 9 and 10 show the CMOD and the geometric correction factor, respectively.

$$CMOD = \frac{6PSaV(\alpha)}{EbD^2} \qquad (9)$$

$$V(\alpha) = 0.76 - 2.26\alpha + 3.87\alpha^2 - 2.04\alpha^3 + \frac{0.66}{(1-\alpha)^2} \qquad (10)$$

For the variable amplitude tests, the stress ratio and R-ratio were changed at different times; the degree of change was commensurate to the degree of damage observed in the specimen. The stress ratios varied between 0.95 and 0.75 and the R-ratios between 0.05 and 0.5. Under random loading, the SR ranged from 0.5 to 0.9 and R-ratio ranged from 0.5 to 0.05.

4 Experimental Results

The results of the fatigue tests are summarized here. Figure 2 shows the log of the crack growth (da/dN) with respect to the crack extension, Δa, for multiple specimens under the three different loading sequences. The crack resistance curve, K_R^f, was obtained by determining the tensile strength f_t', and critical crack opening displacement, w_c, with a similar procedure used for quasi-static loading which involves inverse analysis at the last recorded cycle. The stress parameters c_1 and c_2 were assumed to be the average values obtained under quasi-static loading, 4.6 and 25.3, respectively. The shape parameter m, was also taken to be equal to that obtained under quasi-static loading: 2. The remaining parameters: K_{Rc}^f, Δa_c, λ_1, and λ_2 were determined using the cohesive tensile strength, f_t', and crack opening displacement
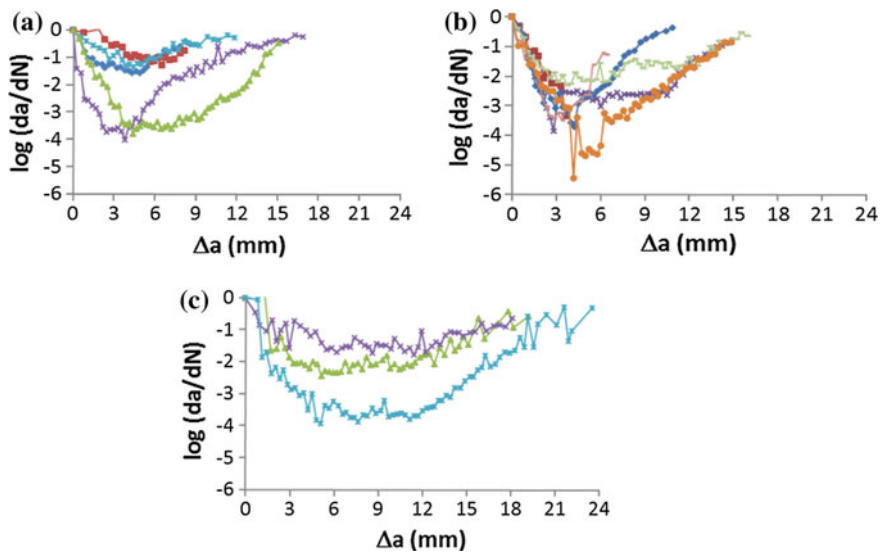
Fig. 2 Crack rate versus crack extension for 100 mm beams under **a** constant, **b** variable, and **c** random loading

Table 2 Summary of test results

Specimen Size	50 mm			100 mm		
	N	$\log C$ (%)	n (%)	N	$\log C$ (%)	n (%)
Constant load	4	-13.2 ± 24	10.5 ± 27	5	-18.4 ± 58	13.4 ± 58
Variable load	10	-23.1 ± 39	18.8 ± 18	9	-24.1 ± 38	18.3 ± 40
Random load	3	-23.4 ± 1	19.4 ± 2	3	-18.6 ± 42	14.1 ± 42
All specimens	17	-20.9 ± 40	16.9 ± 40	17	-21.5 ± 44	16.1 ± 45

using inverse analysis at the last cycle prior to failure. A summary of the Paris parameters determined with and without the use of the fatigue crack resistance curve for both specimen sizes is provided in Table 2. The average tensile strength and crack opening displacement for the 50 mm specimen was: f_t': 4.72 MPa $\pm$ 10 %, w_c: 0.34 mm $\pm$ 25 %, and 100 mm specimens: f_t': 4.39 MPa $\pm$ 14 %, w_c: 0.34 mm $\pm$ 28 %. An Analysis of Variance (ANOVA) analysis was then conducted to assess the statistical significance of the specimen size, D, and loading sequence on the Paris law parameters that were obtained both with and without the fatigue crack resistance curve. Note, the Paris parameters obtained without the use of the fatigue resistance curve means that $K_R^F = 0$ and the modified Paris law is equal to the original Paris law. Under this condition, only data in the accelerating crack region (positive slope regions in Fig. 2) can be evaluated.

The results of the statistical analysis suggest the Paris parameters do not depend on the size or loading sequence when using the modified law (p-value: $\log C$, D: 0.887, *Load*: 0.100; n, D: 0.719, *Load*: 0.071). However, if the fatigue resistance curve is not considered and the Paris law is used, the parameters will depend on specimen size (p-value: $\log C$, D: 0.029, n, D: 0.042) using a 95 % confidence level.

5   Conclusion

The focus of this research was to develop a modified Paris law capable of predicting both crack deceleration and acceleration and also account for size effects. The insertion of a crack resistance curve into the Paris Law can be used to predict non-linear crack growth and account for size effect. When the equivalent fatigue resistance curve is used, on average, the Paris constants are statistically equivalent for two different size specimens under constant, variable, and random amplitude loading, with the fracture parameters $\log C = -20.8$, $n = 16.9$ for 50 mm beams, and $\log C = -21.5$, $n = 16.1$ for 100 mm beams. If the resistance curve is not used, the two Paris constants are not statistically significant under constant, variable, and random amplitude loading, and the fracture parameters are $\log C = -23.71$, $n = 15.60$ for 50 mm beams, and $\log C = -34.3$, $n = 22.0$ for 100 mm beams. It should be noted that the values obtained in this research to calibrate the model are valid for one concrete mix and beam sizes tested. Testing of other mixes and specimen sizes would need to be carried out to check the validity of the approach presented.

References

Bazant ZP, Cedolin L (1984) Approximate linear analysis of concrete fracture by R-curve. ASCE J Structural Engineering 110(6):1336-1355

Bazant ZP, Kazemi MT (1990), Determination of fracture energy, process zone length and brittleness number from size effect, with application to rock and concrete. Int J Fracture 44:111-131

Bazant ZP, Planas J (1998) Fracture and size effect in concrete and other quasi-brittle materials. Boca Raton and London, CRC Press

Brake NA, Chatti K (2012) Prediction of transient and steady state flexural fatigue crack propagation in concrete using a cyclic R-curve. J Engineering Mechanics 138(4):371-378

Brake NA, Chatti K (2013) Prediction of size effect and non-linear crack growth in plain concrete under fatigue loading. Engineering Fracture Mechanics, 109:169-185

Cox BN, Marshall DB (1991) Stable and unstable solutions for bridged cracks in various specimens. Acta Metallurgica et Materiallia 39:579-589

Fett T, Munz D, Geraghty RD, White KW (2000). Bridging stress determination by evaluation of the R-curve. J European Ceramic Society 20(12):2143-2148.

Foote RL, Mai YW, Cotterell B (1986) Crack growth resistance curves in strain softening materials. J Mech Phys Solids 34:593-608

Gallops S, Fett T, Ager III JW, Kruzic JJ (2011) Fatigue threshold R-curves predict small crack fatigue behavior. Acta Materialia 59:7654-7661

Jenq YS., Shah, SP (1985) Two parameter fracture model for concrete. ASCE J. Engineering Mechanics 111(10):1227-1241

Kruzic JJ, Cannon RM, Ager III JW, Ritchie RO (2005) Fatigue threshold R-curves for predicting reliability of ceramics under cyclic loading. Acta Materialia 53(9):2595-2605

Li VC, Matsumoto T (1998) Fatigue crack growth analysis of fiber reinforced concrete with effect of interfacial bond degradation. Cement and Concrete Composites 20:339-351

Mai YW (2002) Cohesive zone and crack-resistance (R)-curve of cementitious materials and their fiber-reinforced composites. J Engineering Fracture Mechanics 69(2):219-234

Miner M (1945) Cumulative damage in fatigue. J. Appl Mechanics 67:A159-A164

Morel S (2007) R-curve and size effect in quasi-brittle fractures: Case of notched structures. J Solids and Structures 44(13):4272-4290

Roesler J, Paulino GH, Park K, Gaedicke, C (2007) Concrete fracture prediction using bilinear softening. Cement Concrete Composites 29:300-312

Subramaniam KV, Oneil EF, Popovics JS, Shah SP (2000) Crack propagation in flexural fatigue of concrete. J Engineering Mechanics 126(9):891-898